Contents lists available at ScienceDirect

Journal of Inorganic Biochemistry

journal homepage: www.elsevier.com

AGHLDDLPGALSAL: A hemoglobin fragment potentially competing with albumin to bind transition metal ions

Giulia Zamariola,[a] Joanna Watly,[b] Eleonora Gallerani,[c] Riccardo Gavioli,[c] Remo Guerrini,[a] Henryk Kozlowski,[b,*] Maurizio Remelli[a,*]

[a] Department of Chemical and Pharmaceutical Sciences, University of Ferrara, via Fossato di Mortara 17, I-44121 Ferrara, Italy
[b] Faculty of Chemistry, University of Wrocław, F. Joliot-Curie 14, 50-383 Wrocław, Poland
[c] Department of Life Sciences and Biotechnology, University of Ferrara, via Luigi Borsari 46, I-44121 Ferrara, Italy

ARTICLE INFO

Article history:
Received 23 December 2015
Received in revised form 14 March 2016
Accepted 3 April 2016
Available online xxx

Keywords:
Metal complexes
Endogenous peptides
AGHLDDLPGALSAL
Complex-formation equilibria
Cytotoxicity of copper

ABSTRACT

Protein degradation leads to the formation of endogenous peptides, the biological activity of which is most often unknown. The peptide AGHLDDLPGALSAL, recently isolated from mouse brain homogenates, has been recognized as a fragment of the α-chain of hemoglobin. AGHLDDLPGALSAL has the ability of inhibiting the peripheral hyperalgesic inflammatory responses through the indirect activation of the μ-opioid receptors. A peculiarity of AGHLDDLPGALSAL is the presence, at its N-terminus of a strong binding site for divalent transition metal ions, similar to that characterizing the human albumin and called "ATCUN motif". The consequential metal binding ability of AGHLDDLPGALSAL can be connected to its biological activity. For this reason, we decided to investigate the coordination properties of AGHLDDLPGALSAL towards Cu(II), Ni(II) and Zn(II) ions, reported here for the first time. The results confirm that AGHLDDLPGALSAL is a strong ligand for those metals: it can even compete with albumin under suitable conditions. *In vitro* assays on the inhibition of Cu(II) toxicity towards different cell lines confirmed that the binding ability of AGHLDDLPGALSAL can imply relevant biological consequences.

1. Introduction

Each organism is characterized by the presence of a set of endogenous peptides (the so-called "peptidome") which derive from the processes of both synthesis and degradation of proteins. These endogenous peptides can be involved in various biological processes, even pathological, for which they can sometimes be considered as biomarkers [1]. The characterization of the human peptidome is then absorbing increasingly relevant efforts by the scientific community [2].

Many human proteins have been recognized for some time as sources of endogenous peptides. These include hemoglobin, from the degradation of the β-chain of which hemorphins derive. Hemorphins are opioid peptides consisting of 4–10 amino acid residues; they have anti-nociceptive activity through activation of opioid receptors and they are also involved in other functions, such as blood-pressure control through the inhibition of the angiotensin binding [3]. On the other hand, from the degradation of the α-chain of hemoglobin, hemopressins instead originate [4], which are able to block the activity of the opioid receptor CB1, with anti-nociceptive and hypotensive effects as well as an action on the appetite control.

Recently, the natural endogenous peptide AGHLDDLPGALSAL, deriving from the α-chain of hemoglobin, was identified in mouse brain homogenates, using a substrate capture assay method combined with isotopic labeling and mass spectrometry [5]. AGHLDDLPGALSAL is formed in the cytosol and possesses the ability of inhibiting the peripheral hyperalgesic inflammatory responses through the indirect activation of the μ-opioid receptors. Since its sequence is also present in other natural peptides, AGHLDDLPGALSAL has been suggested as "the prototype of a new class of bioactive peptides derived from hemoglobin" [5].

The role of AGHLDDLPGALSAL as endogenous peptide acting as a "non-classical neuropeptide", encouraged us to study its coordination properties towards metal ions, never reported so far. In fact, it is worth noticing that its N-terminal sequence (AGH-) corresponds to the well-known ATCUN (Amino Terminal Cu and Ni binding) motif [6], typical of human albumin and characterized by the presence of a histidyl residue in the third position of an N-terminally unprotected peptide. Since AGHLDDLPGALSAL is a natural endogenous peptide, its ability to bind metal ions, in competition with albumin and other low-molecular-weight ligands, cannot be neglected and may have a role in determining the biological activity of the peptide itself [7].

On the basis of the above considerations, the complex-formation equilibria of both AGHLDDLPGALSAL and its short analogue AGHL-Am, protected (amidated) at its C-terminus, with Cu(II), Ni(II) and Zn(II) have been investigated by means of various techniques, including potentiometry and mass spectrometry (for the determination of the stoichiometry and the stability of the formed complexes), UV–visible absorption and circular dichroism (CD) spectrophotometry and electron paramagnetic resonance (EPR) spectroscopy, to obtain information on the structure of the complexes in

* Corresponding authors.
Email addresses: henryk.kozlowski@chem.uni.wroc.pl (H. Kozlowski); maurizio.remelli@unife.it (M. Remelli)

http://dx.doi.org/10.1016/j.jinorgbio.2016.04.001
0162-0134/

solution. In addition, the results of some *in vitro* tests, performed to check the potential protection ability of AGHLDDLPGALSAL against the cell toxicity of Cu(II), are reported.

2. Experimental

2.1. Peptide synthesis

AGHLDDLPGALSAL and AGHL-Am were synthesized according to published methods [8], using Fmoc/*t*-butyl chemistry with a Syro XP multiple peptide synthesizer (MultiSynTech GmbH, Witten Germany). Fmoc-Leu-4-Benzyloxybenzyl alcohol resin (Fmoc-Leu-Wang resin) (0.62 mmol/g, 0.2 g) and 4-(2′,4′-dimethoxyphenyl-Fmoc-aminomethyl)-phenoxyacetamido-norleucyl-methylbenzhydrylamine-resin (Rink amide MBHA resin 0.71 mmol/g, 0.2 g) were employed as starting material. Fmoc protecting group was removed by treatment with 20% piperidine/DMF. Fmoc-amino acids (4-fold excess) were sequentially coupled to the growing peptide chain by using DIPCDI/HOBt (*N*,*N*′-Diisopropylcarbodiimide/1-Hydroxybenzotriazole) (4-fold excess) as activating mixture for 1 h at room temperature. Cycles of deprotection of Fmoc and coupling with the subsequent amino acids were repeated until the desired peptide-bound resin was completed. Peptides were cleaved from the resin using reagent B [9] (trifluoroacetic acid/H20/phenol/triisopropylsilane 88:5:5:2; v/v; 10 mL/0.2 g of resin) for 1.5 h at room temperature. After filtration of the exhausted resin, the solvent was concentrated *in vacuo*, and the residue was triturated with ether, collected by centrifugation and washed three times with cold ether to remove any residual scavengers. Crude peptides were purified by preparative reversed-phase HPLC using a Water Delta Prep 3000 system equipped with a Jupiter column C_{18} (250 × 30 mm, 300 A, 15 μm spherical particle size). The column was perfused at a flow rate of 20 mL/min with a mobile phase containing solvent A (water in 0.1% TFA) and a linear gradient from 0 to 50% of solvent B (60%, v/v, acetonitrile in 0.1% TFA) over 30 min for the elution of peptides. Analytical HPLC analyses were performed on a Beckman 116 liquid chromatograph equipped with a Beckman 166 diode array detector. Analytical purity of the peptides were determined using a Luna C_{18} column (4.6 × 100 mm, 3 μm particle size, Phenomenex) with the above solvent system (solvents A and B) programmed at a flow rate of 0.5 mL/min and a linear gradient from 0% to 30% B over 25 min. Both the peptides showed a purity > 95% when monitored at 220 nm. Molecular weight of the final purified peptides was checked with an ESI Waters-Micromass ZMD-2000 instrument.

2.2. Potentiometric measurements

Stability constants for proton and metal complexes were measured by means of potentiometric titration curves registered over the pH range 3–11, using a total volume of about 1.5 mL (exactly determined by weighting the solution and correcting for the water density at the room temperature). The pH-metric titrations were performed with a Molspin pH meter equipped with a MettlerToledo InLab semi-combined electrode, calibrated in hydrogen ion concentration using HCl [10]. Alkali was added with a 0.250 mL micrometer syringe, previously calibrated by both weight titration and the titration of standard materials. Constant-speed magnetic-stirring was applied throughout. The room temperature was kept at 298.2 ± 0.2 K. High purity grade argon was gently blown over the test solution, in order to maintain an inert atmosphere, after bubbling in a solution of identical temperature and ionic strength of the sample. The ligand concentration was about $0.6 \cdot 10^{-3}$ M and the metal-to-ligand ratio was 0.9:1. $CuCl_2$, $NiCl_2$ and $ZnCl_2$ were highly pure products (Sigma-Aldrich); the concentration of their stock solutions was determined by ICP-MS. The carbonate-free stock solution of NaOH 0.1 M was purchased from Sigma-Aldrich and then potentiometrically standardized with potassium hydrogen phthalate as primary standard. The HCl stock solution was prepared by diluting concentrated HCl (Sigma-Aldrich) and then standardized with NaOH. All sample solutions were prepared with freshly doubly distilled water. The ionic strength was adjusted to 0.1 M by adding KCl (Sigma-Aldrich). Grade A glassware was employed throughout.

The standard potential and the slope of the electrode couple were computed by means of the GLEE [11] or SUPERQUAD [12] programs. The purities and the exact concentrations of the ligand solutions were determined either by the Gran method [13] or by using the SUPERQUAD program. The HYPERQUAD program [14] was employed for the calculation of the overall (β) stability constant, referred to the following equilibrium:

$$pM + qL + rH \rightleftarrows M_pL_qH_r$$

(charges omitted; p might also be 0 and r can be negative). The associated standard deviations (referring to random errors only), are reported in parentheses in the tables as uncertainties on the last significant figure.

The stability constants of complexes with different stoichiometry and protonation degree cannot be directly compared. The most popular parameters used to evaluate (and compare) the global binding ability of a ligands towards a metal ion, under given experimental conditions (i.e. at physiological pH) are the dissociation constant (K_d) [15] and the pM value [16]. The former refers to a hypothetical overall equilibrium:

$$M + L \rightleftarrows ML$$

where the protonation degree of the ligand (and the complex) is not explicitly considered. The second parameter is the negative logarithm of the concentration of the free metal ion (pM), in the presence of the ligand, under normalized experimental conditions, i.e. $[L]_{total} = 10^{-5}$ M and $[M]_{total} = 10^{-6}$ M, at pH 7.4. In addition, the comparison can be extended to the whole explored pH range by computing and plotting the "competition diagrams". These graphs are calculated by simulating a solution containing both the considered metals and the ligands and assuming that mixed complexes are not formed. These competition diagrams have the purpose to compare qualitatively the ligand-to-metal affinity on the entire pH range, regardless of the stoichiometry and the structure of the formed species. The speciation and competition diagrams as well as the K_d values, were computed with the HYSS program [17]. The equilibrium constants for the hydrolysis of metal cations were taken from the literature [18,19].

2.3. Spectroscopic measurements

The absorption spectra were recorded with a Varian Cary 300 Bio spectrophotometer, in the range 200–800 nm, using a quartz cuvette with an optical path of 1 cm. Circular dichroism (CD) spectra were recorded on Jasco J 715 spectropolarimeter in the 225–800 nm range, using a quartz cuvette with an optical path of 1 cm in the visible and near-UV range or with a cuvette with an optical path of 0.1 cm in the wavelength range under 300 nm. CD spectra were processed using Jasco Spectra Analysis Software (version 1.53.04). Electron paramagnetic (EPR) spectra were recorded in liquid nitrogen on a Bruker ESP ELEXSYS E500 CW-EPR spectrometer at X-band frequency (9.5 GHz) and equipped with ER 036TM NMR Teslameter and E41

FC frequency counter. 25% ethylene glycol was used as a cryoprotectant for EPR measurements. The EPR experimental parameters are reported as Supplementary information (Table S1). The EPR spectroscopic parameters were obtained by computer simulation of the experimental spectra using WIN-EPR SimFonia program, version 1.26 (Bruker Analytik GmbH).

The concentration of solutions used for spectroscopic studies were similar to those employed in the potentiometric experiment. The UV–Vis and CD spectroscopic parameters were calculated from the spectra obtained at the pH values corresponding to the maximum concentration of each particular species, on the basis of distribution diagrams and using the Origin 7.0 program.

2.4. Mass spectrometric measurements

High-resolution mass spectra were obtained on a Bruker MicrOTOF-Q spectrometer BrukerDaltonik (Bremen, Germany), equipped with an Apollo II electrospray ionization source with an ion funnel. The mass spectrometer was operated both in the positive and in the negative ion modes. The instrumental parameters were as follows: scan range *m*/*z* 250–2000, dry gas–nitrogen, temperature 473 K, and ion energy 10 eV. Capillary voltage was optimized to the highest S/N ratio and it was 4500 V. The samples were prepared in MeOH and measured pH value was approximately 5.3. The sample was infused at a flow rate of 3 μL/min. The instrument was calibrated externally with the Tunemix™ mixture (BrukerDaltonik, Germany) in quadratic regression mode. Data were processed by using the Bruker Compass DataAnalysis 4.0 program. The mass accuracy for the calibration was better than 5 ppm, enabling together with the true isotopic pattern (using SigmaFit) an unambiguous confirmation of the elemental composition of the obtained complex.

2.5. Cellular assays

In order to assess the level of toxicity of copper on cells and the ability of the AGHLDDLPGALSAL peptide to limit this toxicity, MTT (3-(4,5-dimethylthiazol-2-yl)-2,5-diphenyltetrazolium bromide) assays [20] were carried out on three different cell lines: K562, A2780 and human fibroblasts. MTT assays were performed in medium (RPMI - Roswell Park Memorial Institute medium or DMEM - Dulbecco's Modified Eagle Medium, depending on the cell line considered) without fetal calf serum (FCS) to avoid the presence of albumin which has high sequence homology with the AGHLDDLPGALSAL peptide. Thus, the absence of FCS avoids the aspecific capture of the cupric ion by albumin. K562 and A2780 cells were seeded in triplicate in 96-well plates at a density of $25 \cdot 10^3$ cells/well in RPMI while human fibroblasts were seeded at a density of $5 \cdot 10^3$ cells/well in DMEM. Cells were treated for 24 h with different concentrations of $CuCl_2$ (50 μM, 100 μM and 200 μM) in the presence or not of the same dose of the AGHLDDLPGALSAL peptide. Cells treated with an irrelevant peptide (NAIVFKGL) were used as a negative control and taken as reference of 100% of cell proliferation.

After treatment, 25 μL of a 12 mM solution of MTT were added for 2 h followed by the addition of 100 μL of lysing buffer (50% dimethylformamide + 20% sodium dodecyl sulfate, pH 4.7) to dissolve formazan product. After additional 18 h the solution absorbance, proportional to the number of live cells, was measured by spectrophotometer at 570 nm and converted into % of growth inhibition.

3. Results

3.1. Protonation equilibria

AGHLDDLPGALSAL is fully unprotected and presents five protonable sites: the amino group of the terminal Ala, the side imidazole group of His and the three carboxyl groups of two Asp residues and the C-terminal Leu. The ligand completely deprotonated (conventionally employed to indicate the stoichiometry of the species in solution) bears three negative charges (L^{3-}). On the other hand, its short analogue AGHL-Am lacks the three carboxylic groups and its unprotonated form (L) is neutral.

The protonation constants are reported in Table 1 while the corresponding distribution diagrams are reported as Supplementary Information (Fig. S1).

On the basis of the literature for similar peptides [21], it is not difficult to attribute the pK_a values to the five acid or basic groups, as shown in Table 1. Only in the case of the two Asp residues, it is not possible to exactly distinguish between the two sites, although it can be suggested that the most acidic one is that in position 5, i.e. that closer to His which is protonated and positively charged in the pH range where deprotonation of Asp residues occurs. A similar effect can also explain the lower pK_a values found for amine and imidazole residues of AGHL-Am with respect to its longer analogue: in this case the reason is the absence of the C-terminal tail of AGHLDDLPGALSAL, which is triply negatively charged in the pH range where protonation equilibria of AGHL-Am take place.

3.2. Cu(II) complexes

Both AGHLDDLPGALSAL and AGHL-Am contain a His residue in the third position of their N-terminus, which is unprotected: this sequence of three amino acids constitutes the well-known "ATCUN motif", an excellent binding site for the Cu(II) ion [6]. In addition, in the case of AGHLDDLPGALSAL, also the C-terminus is unprotected and its carboxylic group, as well as the other two carboxylic groups of the Asp residues, can participate in the metal binding. Furthermore, other available donor atoms are the nitrogens of the polypeptide backbone: in fact, it is well-known that copper, already at moderately acidic pH, can displace the proton of the amide group (which instead, in the absence of metal ions, has a logK_a value close to 15 [22]).

In the metal-to-ligand equimolar solutions explored here, AGHLDDLPGALSAL forms four mononuclear Cu(II) complexes with stoichiometry [CuLH], $[CuLH_{-1}]^{2-}$, $[CuLH_{-2}]^{3-}$,

Table 1.
Protonation constants for the peptides AGHLDDLPGALSAL and AGHL-Am, at T = 298 K and I = 0.1 M (KCl).

Peptide	Species	Logβ	pK_a	Residue
AGHLDDLPGALSAL	LH^{2-}	8.23 (3)	8.23	N-terminus
	LH_2^{-}	14.78 (5)	6.55	His
	LH_3	18.89 (6)	4.11	Asp
	LH_4^{+}	22.62 (6)	3.73	Asp
	LH_5^{2+}	25.07 (8)	2.45	C-terminus
AGHL-Am	LH^{+}	7.82 (1)	7.82	N-terminus
	LH_2^{2+}	14.02 (1)	6.20	His

and $[CuLH_{-3}]^{4-}$. In Table 2, the complex-formation constants are reported; the corresponding distribution diagrams are drawn in Fig. 1. The 1:1 stoichiometry is confirmed by MS spectra reported as Supplementary Information (Fig. S2). Neither potentiometry nor mass spectrometry support the formation of bis-complexes or polynuclear species, under the present experimental conditions.

Spectrophotometric (UV–Vis, CD) data recorded on the system Cu(II)/AGHLDDLPGALSAL are shown in Table 3 and Fig. 2, while EPR results are reported as Supplementary Information (Table S2 and Fig. S3): a low UV–Vis absorption and weak CD signals were obtained at pH lower than 5. On the contrary, at pH > 5, where the $[CuLH_{-2}]^{3-}$ complex predominates (see Fig. 1a), the spectra are intense and almost identical at every pH.

Table 2.
Cu(II) complex-formation constants with AGHLDDLPGALSAL and AGHL-Am, at T = 298 K and I = 0.1 M (KCl).

Peptide	Species	Logβ	pK_a
AGHLDDLPGALSAL	[CuLH]	13.90 (3)	–
	$[CuLH_{-1}]^{2-}$	4.62 (2)	4.87
	$[CuLH_{-2}]^{3-}$	− 0.25 (3)	9.38
	$[CuLH_{-3}]^{4-}$	− 9.63 (6)	–
AGHL-Am	$[CuLH_{-1}]^{+}$	2.8 (2)	3.12
	$[CuLH_{-2}]$	− 0.33 (1)	10.67
	$[CuLH_{-3}]^{-}$	− 10.99(3)	–

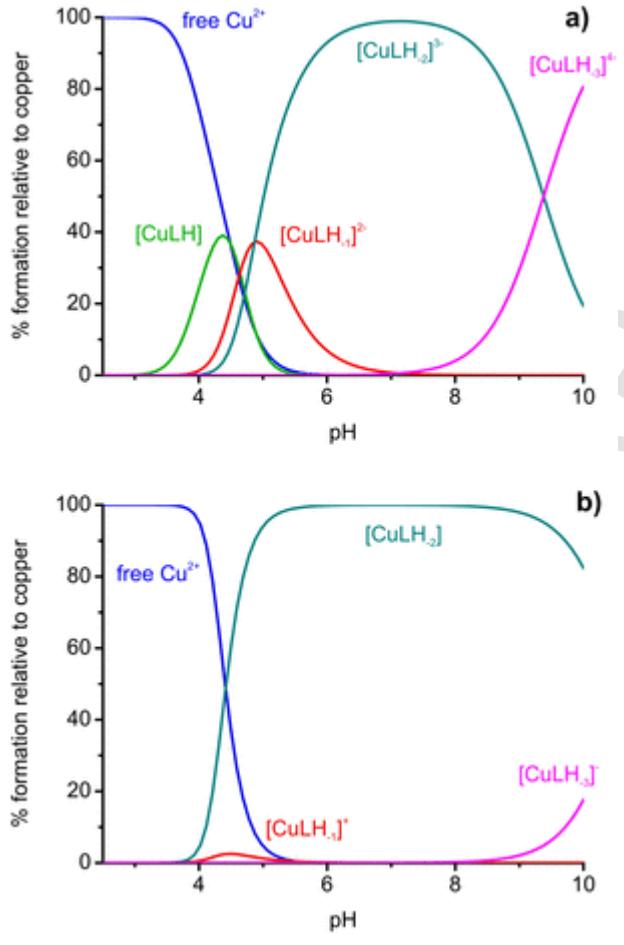

Fig. 1. Representative distribution diagrams for the complex-formation of Cu(II) with: a) AGHLDDLPGALSAL and b) AGHL-Am. Temperature 298 K and I = 0.1 M (KCl). $C°_M = 0.5 \cdot 10^{-3}$ M; M/L molar ratio = 0.9.

Table 3.
Spectrophotometric parameters at different pH values for the system Cu(II)/AGHLDDLPGALSAL; $C°_{Cu} = 0.5 \cdot 10^{-3}$ M; M/L ratio = 0.9.

pH	Species	Vis		CD	
		λ/nm	ε/M^{-1} cm^{-1}	λ/nm	$\Delta\varepsilon$/M^{-1} cm^{-1}
4.5	[CuLH], $[CuLH_{-1}]^{2-}$	537	18	–	–
5.2	$[CuLH_{-1}]^{2-}$, $[CuLH_{-2}]^{3-}$	522	86	258	0.08
				274	− 0.25
				305	0.35
				499	0.52
				580	− 0.10
6.2	$[CuLH_{-2}]^{3-}$	522	97	254	0.07
				271	− 0.28
				304	0.58
				497	0.75
				581	− 0.16
7.2	$[CuLH_{-2}]^{3-}$	522	106	251	0.08
				272	− 0.30
				303	0.62
				497	0.76
				580	− 0.17
8.1	$[CuLH_{-2}]^{3-}$	522	106	255	0.21
				273	− 0.37
				305	0.68
				496	0.72
				581	− 0.18
9.2	$[CuLH_{-2}]^{3-}$, $[CuLH_{-3}]^{4-}$	522	118	253	0.21
				272	− 0.35
				307	0.69
				497	0.74
				580	− 0.26
10.3	$[CuLH_{-3}]^{4-}$	527	123	253	0.20
				271	− 0.32
				304	0.69
				496	0.72
				581	− 0.27

AGHLDDLPGALSAL starts binding the Cu(II) ion at pH 3, forming the neutral complex [CuLH], which reaches its maximum concentration around pH 4.3. Mainly due to the overlap with the free (hexaaquo) copper ion, it was not possible to accurately determine the spectroscopic parameters of the complex [CuLH]. The stoichiometry of this species implies that one site of the ligand is protonated. It is worthy of note that in Cu(II) complexes of the ATCUN type with tetrapeptides like KGHK [23] or AGHL-Am (Table 2 and Fig. 1b) this protonated species is not observed while with tripeptides like GGH [24] or DAH [25] it is formed only in a very low amount. In the latter cases, the logβ values of the protonated species are 12.40 and 12.85, respectively, while in the case of AGHLDDLPGALSAL a value of 13.90 was measured and the [CuLH] complex reaches the amount of 40% of involved Cu(II) (Fig. 1a). The peculiarity of AGHLDDLPGALSAL with respect to the above short peptides is the presence of two Asp residues sufficiently close to His to participate in complex-formation and stabilization. This could be the main reason of the higher stability (1–1.5 orders of magnitude) of the [CuLH] complex of AGHLDDLPGALSAL. An additional reason could be a more favorable entropic contribution due to charge neutralization in the formation of this complex, causing the releasing of water molecules from the solvation spheres of the reagents/product; on the contrary, in the case of the peptides GGH and DAH, the monoprotonated complex is positively charged.

The second species detected, $[CuLH_{-1}]^{2-}$, begins to form around pH 4.0 and reaches its maximum at pH 5. This species derives from the previous complex from which two protons are released simultaneously or in a so rapid sequence do not to allow the detection of the intermediate species $[CuL]^{-}$. The stoichiometry of the complex $[CuLH_{-1}]^{2-}$ indicates that all the acidic and basic sites of the side

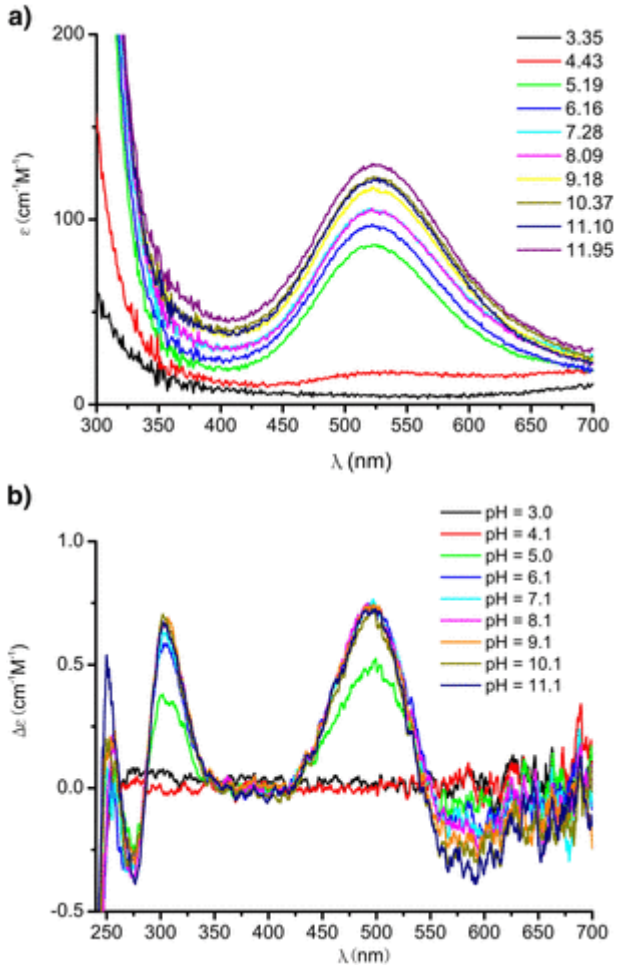

Fig. 2. Vis (top) and CD (bottom) spectra, at different pH values, for the system Cu(II)/AGHLDDLPGALSAL; $C°_{Cu} = 0.5 \cdot 10^{-3}$ M; M/L ratio = 0.9.

chains are deprotonated and an additional proton has been displaced by the metal ion. Since the pH range of formation of this species is too low to allow the spontaneous deprotonation of both the amino and imidazole groups, they should be coordinated to the metal. The additional proton can only be released from an amide nitrogen (N_{am}^-) of the peptide chain, which must also be bound to copper, because its pK_a value, in the absence of metal, is very high. Taken together, these considerations suggest that the complex $[CuLH_{-1}]^{2-}$ has a coordination 3N, with equatorial donor atoms (NH_2, N_{am}^-, N_{im}), where N_{im} denotes the imidazole nitrogen. Also in this case the formation constant of this species (4.62, Table 2) is markedly higher than that measured for the short model peptides: 2.55 for GGH [24] and 2.6 for AHGL-Am (Table 2), suggesting that at least one carboxylate group of the Asp residue is still bound to copper ion.

Starting from pH 4.5 and almost simultaneously to the species $[CuLH_{-1}]^{2-}$, the complex $[CuLH_{-2}]^{3-}$ is formed; it is the major species between pH 5 and pH 9 and the only species present in solution at physiological pH. The pK_a value for the species $[CuLH_{-1}]^{2-}$ (4.87) is compatible with the deprotonation of a second nitrogen atom of the peptide backbone with its involvement in the complexation of Cu(II) and the formation of a complex 4N, with equatorial donor atoms (NH_2, $2N_{am}^-$, N_{im}). Coordination 4N is confirmed by the experimental parameters of the Vis absorption, CD and EPR spectra (Tables 3 and S2), characteristic of a strong ligand field around the metal ion. It is worth of note how the spectra remain virtually unchanged (apart from their intensity) from pH 5 to pH 11, as already reported in the numerous previous studies on the Cu(II) coordination of ATCUN peptides [23,26–29]. The presence of the Cu(II)-amine, Cu(II)-imidazole and Cu(II)-amide coordination bonds is confirmed by the intense bands of the UV-CD spectrum around 250 nm, 270 nm and 305 nm, respectively. The stability constant of the complex $[CuLH_{-2}]^{3-}$ with AGHLDDLPGALSAL (− 0.25, Table 2) is markedly higher than that reported for the analogous species ($[CuLH_{-2}]^-$) of GGH (− 1.55) [24], suggesting that one Asp carboxylate is still bound to copper in apical position, thus giving an extra-stabilization contribution. On the other hand, the stability constant of the complex $[CuLH_{-2}]^{3-}$ with AGHLDDLPGALSAL is very close to that of the corresponding $[CuLH_{-2}]$ species of AGHL-Am (− 0.33, Table 3) where no additional donor atom is available, besides the four nitrogens already bound to the equatorial plane of the complex. In this case the charge difference could be again the cause of a favorable entropic contribution to the stability of the neutral $[CuLH_{-2}]$ complex formed by AGHL-Am.

Between pH 7.5 and 9, a further deprotonation step takes place in both the systems here investigated, without substantial changes in the spectroscopic properties of the solution; this suggests that the coordination geometry around the metal does not change. The proton released could derive from an axial water molecule: the corresponding proton-dissociation constant and the moderate red-shift observed in the Vis spectra at pH higher than 10 support this hypothesis.

3.3. Ni(II) complexes

Potentiometric results concerning Ni(II) complexes with AGHLDDLPGALSAL and AGHL-Am are reported Table 4; data processing was limited to the pH range 3.5–8.0 since at basic pH the kinetics of complexation becomes very slow and the electrode signal was unstable also 1 h after the addition of the titrant.

The formation of the nickel complexes begins around pH 5 (two units higher than copper), as shown in the distribution diagrams of Fig. 3; both potentiometry and MS agree on the 1:1 stoichiometry (see Fig. S4, Supplementary Information). The first species to form with both AGHLDDLPGALSAL and AGHL-Am is the complex $[NiLH_{-1}]^{2-}$; in the case of the tetrapeptide, the stoichiometry is the same, but the charge is positive. The corresponding formation constants are about four orders of magnitude lower than those obtained with copper. Since not only Cu(II) but also Ni(II) ions are able to deprotonate and bind the amide nitrogens of the peptide backbone [30], the donor atom set of these nickel complexes is most likely the same of the corresponding copper species, i.e. (NH_2, N_{am}^-, N_{im}), with an octahedral coordination geometry. The higher stability of the complex formed by AGHLDDLPGALSAL with respect to that formed by AGHL-Am can again be explained with the participation of one or more carboxylates of Asp residue, certainly deprotonated in the pH range of existence of these complexes.

Table 4.
Ni(II) complex-formation constants with AGHLDDLPGALSAL and AGHL-Am, at T = 298 K and I = 0.1 M (KCl).

Peptide	Species	Logβ	pK_a
AGHLDDLPGALSAL	$[NiLH_{-1}]^{2-}$	0.55 (7)	6.63
	$[NiLH_{-2}]^{3-}$	− 6.08 (9)	–
AGHL-Am	$[NiLH_{-1}]^{+}$	− 0.41 (6)	5.00
	$[NiLH_{-2}]$	− 5.41 (1)	–

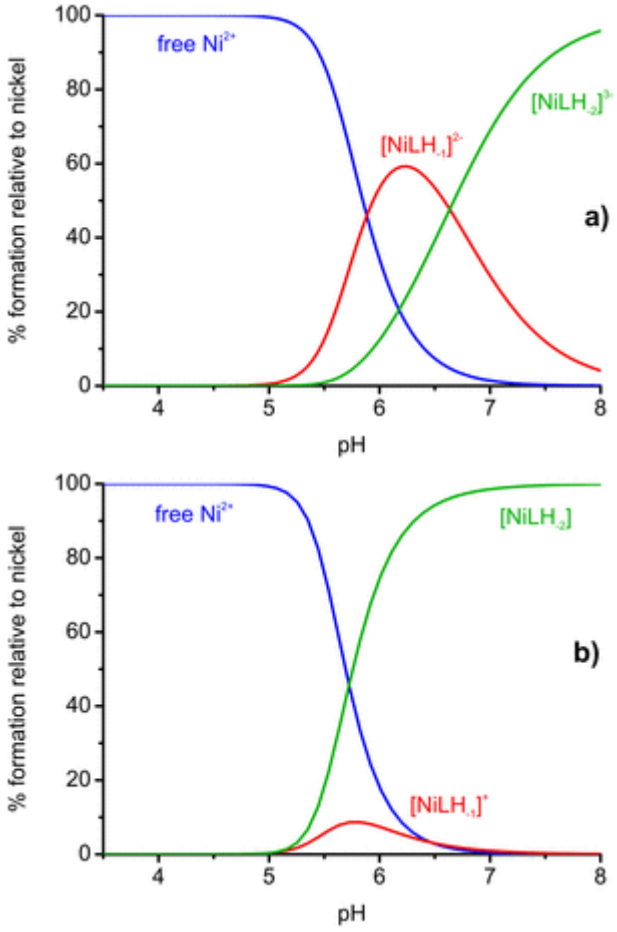

Fig. 3. Representative distribution diagrams for the complex-formation of Ni(II) with: a) AGHLDDLPGALSAL and b) AGHL-Am. Temperature 298 K and I = 0.1 M (KCl). $C°_M = 0.5 \cdot 10^{-3}$ M; M/L molar ratio = 0.9.

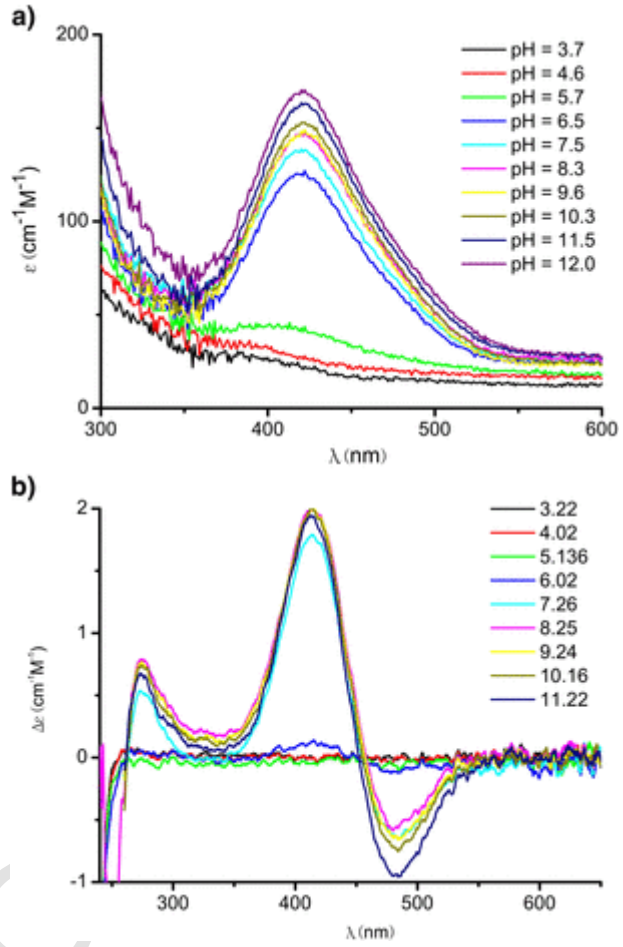

Fig. 4. Vis (top) and CD (bottom) spectra, at different pH values, for the system Ni(II)/AGHLDDLPGALSAL; $C°_{Cu} = 0.5 \cdot 10^{-3}$ M; M/L ratio = 0.9.

The second Ni(II) species has the stoichiometry 11–2 ($[NiLH_{-2}]^{3-}$ for the long peptide and $[NiLH_{-2}]$ for the tetrapeptide) and it is characterized by a logβ value which is 6 logarithmic units lower than that measured with Cu(II); this complex begins to form around pH 5.5 and it is the dominant species at neutral and basic pH. The differences in affinity for the peptides towards Cu(II) and Ni(II) are in agreement with what normally found in the literature [21]. It is worth of note that, increasing the pH, the solution becomes yellow due to a strong absorption in the d-d region, thus suggesting the formation of a square planar complex of Ni(II) [31–33]. As shown in Fig. 4, the wavelength of maximum absorption at pH higher than 6.5 is about 420 nm, in agreement with a 4N co-ordination (NH_2, $2N^-$, N_{im}) [34]. In the CD spectra, in addition to the dual-band relative to the d-d transitions localized around 450 nm, an intense positive band at 260–270 nm, attributable to the coordination of amide and/or imidazole nitrogens to nickel is observed [35]. Although shifted at lower wavelength, CD spectra have the same shape of those recorded with Cu(II) (Fig. 2), as expected for a complex with an "ATCUN peptide" [30]. At pH higher than 8, both Vis and CD spectra do not change, suggesting that the same coordination geometry is maintained by the nickel complex.

3.4. Zn(II) complexes

The complex-formation equilibria with the zinc ion were analyzed only by potentiometry and mass spectrometry, since Zn(II) is spectrophotometrically inactive. At pH higher than 8.5 zinc hydrolysis with precipitation was observed. The stability constants values are reported in Table 5 while the corresponding distribution diagrams are shown in Fig. 5.

The formation of zinc complexes starts around pH 5.5 for both the peptides. Only mononuclear species have been detected, as confirmed by ESI-MS spectra (see Fig. S5, Supplementary information). The Zn(II) ion is generally considered unable to displace the amide protons [36]: therefore, the complex-formation should only involve the imidazole group of histidine, the terminal amine group and the carboxylic groups present in the sequence.

In the case of AGHLDDLPGALSAL, potentiometric titrations revealed the formation, at acid/neutral pH, of the protonated bis-com-

Table 5.
Zn(II) complex-formation constants with AGHLDDLPGALSAL and AGHL-Am, at T = 298 K and I = 0.1 M (KCl).

Peptide	Species	Logβ
AGHLDDLPGALSAL	$[ZnL_2H_2]^{2-}$	22.8 (5)
	$[ZnL]^-$	4.56 (9)
	$[ZnLH_{-2}]^{3-}$	− 12.16 (9)
AGHL-Am	$[ZnL]^{2+}$	3.36 (2)
	$[ZnLH_{-2}]$	− 12.08 (2)

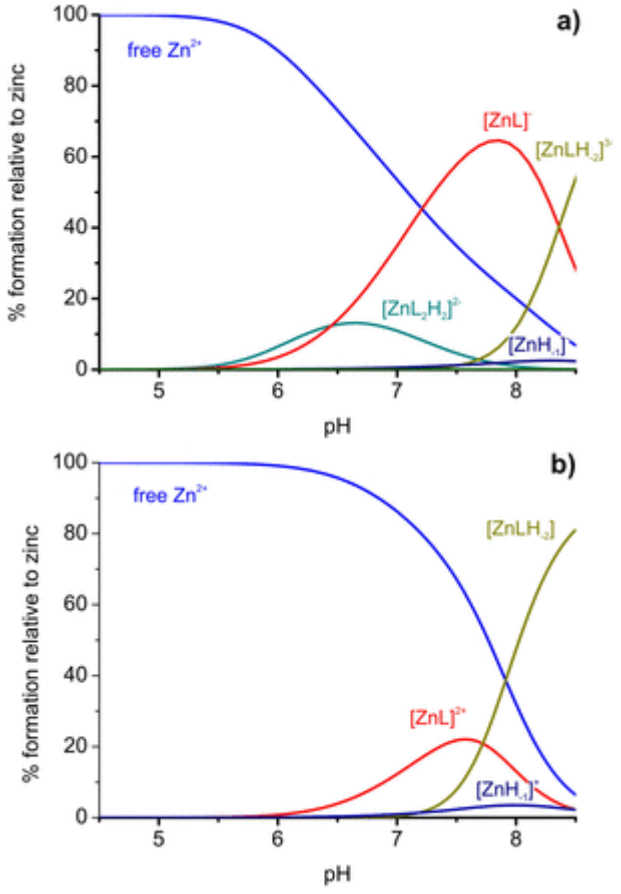

Fig. 5. Representative distribution diagrams for the complex-formation of Zn(II) with: a) AGHLDDLPGALSAL and b) AGHL-Am. Temperature 298 K and I = 0.1 M (KCl). $C°_M = 0.5 \cdot 10^{-3}$ M; M/L molar ratio = 0.9.

plex $[ZnL_2H_2]^{2-}$. This species could not be observed in the mass spectra, most likely because it forms in low amount. The stoichiometry suggests that two mono-protonated ligands are coordinated to the metal: within the pH range of formation of the complex $[ZnL_2H_2]^{2-}$ (5.3–8.2) the unique site that can be protonated is the terminal amino group. As a consequence, in this bis-complex, most likely of tetrahedral geometry, each peptide should be linked to Zn(II) via the imidazole group of His; in addition, the stability constant value (22.8, Table 5) suggests that one carboxylic group of the ligand participates in complexation. In fact, taking into account the protonation constant of AGHLDDLPGALSAL at the terminal amine (8.23, Table 1) and the formation constant of a Zn(II)-imidazole complex, under the same experimental conditions (2.56, [37]) a computed value of 21.58 could be predicted for the logβ value of $[ZnL_2H_2]^{2-} > 1$ order of magnitude lower than the experimental value. This difference can be ascribed to the stabilizing effect due to the additional coordination of one carboxylate. It is not possible to establish if this carboxylate is that of the free C-terminus of one of the side groups of Asp residues, although the latter hypothesis looks more likely.

Starting from pH 5.5, the unprotonated mono-complex $[ZnL]^-$ ($[ZnL]^{2+}$ in the case of AGHL-Am) is formed; this is the most abundant species at physiological pH, although its concentration is never higher than 25% of total zinc for AGHL-Am. The stoichiometry of this complex requires that both the imidazole and the terminal amino nitrogens are unprotonated and bound to the metal ion, forming a (NH_2, N_{im}) species. While, for AGHL-Am, the two remaining positions of the tetrahedron can be only occupied by water molecules, in the case of AGHLDDLPGALSAL some carboxylate groups are also available for coordination. The difference between the formation constants of this complex formed by the two peptides suggests that this is the case. In fact, the log$\beta_{[ZnL]}$ value for AGHL-Am is 3.36 (Table 5), quite close to the literature value reported for the same species in the system Zn(II)/GGH [3.31, [38]], but one order of magnitude lower than that measured for AGHLDDLPGALSAL (4.56, Table 5). In turn, the latter is close to the constant found for the same species in the system Zn(II) and the N-terminal domain of human albumin, i.e. the protected model tripeptide Asp-Ala-His-Amide (DAH-Am), (4.17, [39]) also containing a side carboxylic group available for coordination.

Finally, in the alkaline pH range, the doubly deprotonated complex $[ZnLH_{-2}]^{3-}$ ($[ZnLH_{-2}]$ for AGHL-Am) is formed. The stability constants are almost identical for the two peptides, suggesting the same geometry: Zn(II) is bound to the bidentate (NH_2, N_{im}) ligand and to two hydroxyl ions.

3.5. Cellular assays

To evaluate the capacity of AGHLDDLPGALSAL to inhibit Cu-mediated cell toxicity, K562 and A2780 tumor cells, and human fibroblasts were cultured in a medium containing increasing concentrations of $CuCl_2$ in the presence or not of AGHLDDLPGALSAL. As shown in Fig. 6, the toxicity of copper chloride alone on K562 cells is dose dependent and 70% of cell toxicity was observed in the presence of 200 μM $CuCl_2$. On the other hand, the AGHLDDLPGALSAL peptide alone does not show any toxicity. However, the addition of equimolar concentrations of AGHLDDLPGALSAL decreases Cu-induced toxicity to 20%. The presence of an irrelevant control peptide, administered either alone or together with copper chloride, has no effect, confirming the specificity of AGHLDDLPGALSAL against copper.

Similar results were obtained on A2780 tumor cells. As shown in Fig. 7, the AGHLDDLPGALSAL peptide alone as well as the irrelevant control peptide (the latter administered either alone or together with copper chloride) have no effect. On the other hand, the presence of AGHLDDLPGALSAL inhibits Cu-induced cell toxicity of about 20%.

As shown in Fig. 8, the copper toxicity on human fibroblasts shows profiles similar to those determined on tumor cells, although with lower values, corresponding to the 45% cell toxicity. The presence of AGHLDDLPGALSAL alone shows no toxicity, while the presence of AGHLDDLPGALSAL in association with $CuCl_2$ lowers the toxicity levels of the metal ion of > 20%. As observed with tumor cells, the presence of the irrelevant peptide does not influence the toxicity of copper.

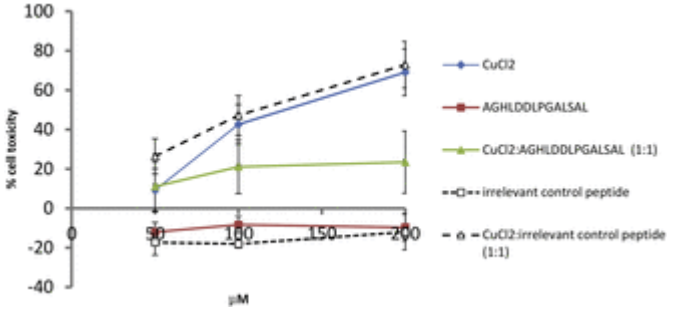

Fig. 6. MTT assay on 25,000 K562 cells, expressed as percentage of cell toxicity. Average of three separate experiments, with indication of the standard error.

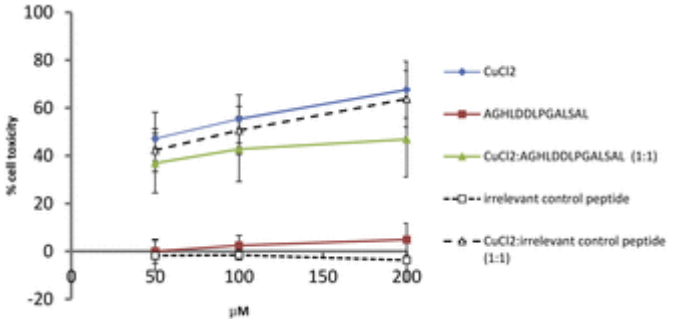

Fig. 7. MTT assay on 25,000 A2780 cells, expressed as percentage of cell toxicity. Average of three separate experiments, with indication of the standard error.

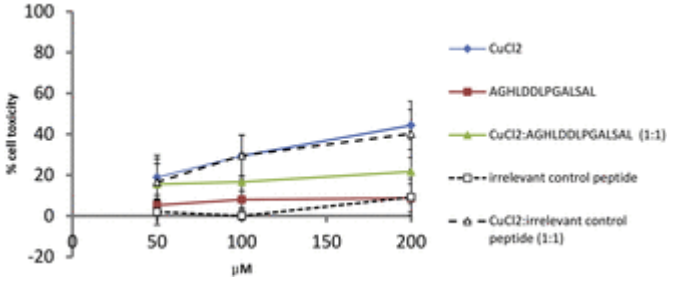

Fig. 8. MTT assay of 5000 human fibroblasts (plated at the day − 1), expressed as a percentage of cell toxicity. Average of three separate experiments, with indication of the standard error.

All these experiments lead to the conclusion that the peptide AGHLDDLPGALSAL reduces the toxicity due to copper from 20 to almost 50% depending on the considered cell line.

4. Discussion

In order to compare the relative stability of the complexes formed by different ligands with the same metal ion or, *vice versa*, by a ligand with different metal ions, it is useful to calculate the corresponding K_d constant values (Table 6) and to build up some competition diagrams (Figs. 9-12). While K_d can be useful to compare the metal-peptide affinities (at physiological pH) of systems investigated with different experimental procedures, without exactly define the complete speciation model, the competition diagrams allow a wide comparison throughout all the explored pH range.

In agreement with the literature, the affinity of a peptide containing the ATCUN-site for the metal cations studied here decreases in the order: Cu(II) ≫ Ni(II) - although the coordination geometry is the same for the two metals - and Ni(II) ≫ Zn(II), because of the inability of zinc to bind the amide nitrogens of the peptide backbone by displacing the nitrogen protons. In the case of AGHLDDLPGALSAL, this behavior is clearly shown by the competition diagrams of Fig. 9a (where all the three metals are taken into account) and Fig. 9b (where instead the comparison is limited to nickel and zinc) and reflected in the K_d values of Table 6. A similar behavior was found also in the case of AGHL-Am (see Fig. S6, Supplementary information).

Table 6.
Calculated dissociation constants (K_d/M^{-1}) for Cu(II), Ni(II) and Zn(II) complexes with AGHLDDLPGALSAL, AGHL-Am and short peptides taken as models for the human albumin N-terminal binding site.

Peptide/metal ion	Cu(II)	Ni(II)	Zn(II)	Data from
AGHLDDLPGALSAL	$2.43 \cdot 10^{-14}$	$1.42 \cdot 10^{-8}$	$1.80 \cdot 10^{-4}$	This work
AGHL-Am	$1.29 \cdot 10^{-14}$	$1.54 \cdot 10^{-9}$	$1.35 \cdot 10^{-3}$	This work
DAHK-Am	$1.69 \cdot 10^{-14}$	$1.85 \cdot 10^{-9}$	–	[40]
DAH-Am	–	–	$1.68 \cdot 10^{-4}$	[41]

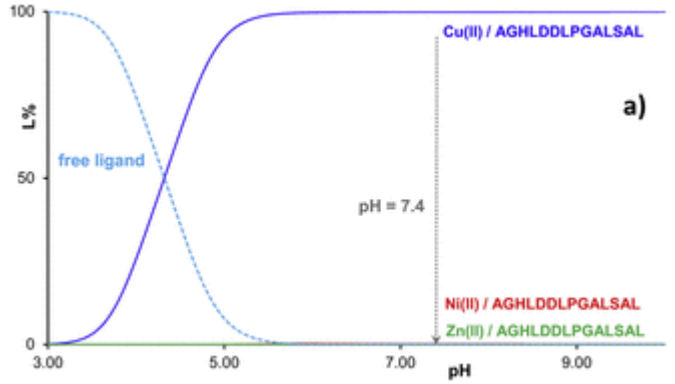

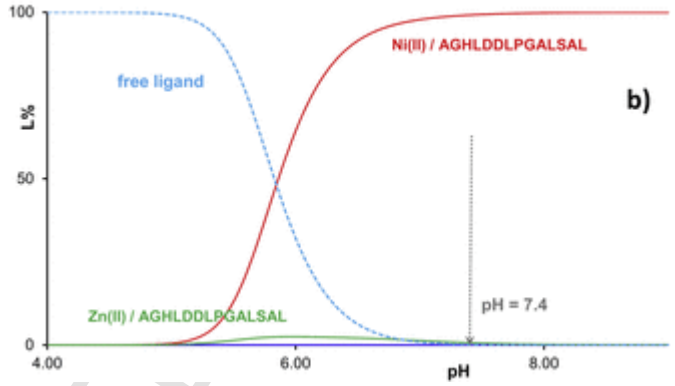

Fig. 9. Competition diagrams calculated for solutions containing equimolar amounts of: a) Cu(II), Ni(II), Zn(II) and AGHLDDLPGALSAL; b) Ni(II), Zn(II) and AGHLDDLPGALSAL.

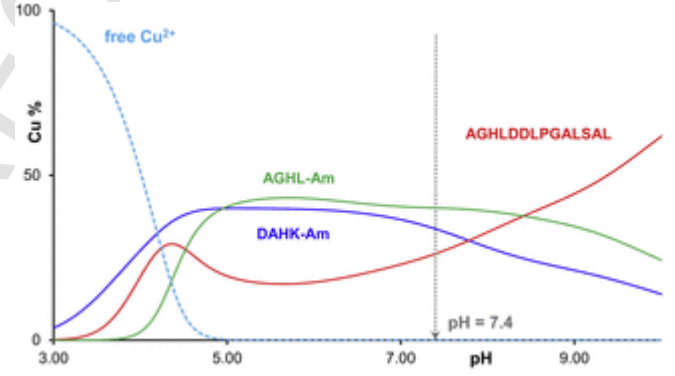

Fig. 10. Competition diagram calculated for a solution containing AGHLDDLPGALSAL, its short analogue AGHL-Am, the peptide DAHK-Am and Cu(II) in equimolar amounts. Stability constant data for DAHK-Am are taken from [40].

In order to shed light on the possible biological role of AGHLDDLPGALSAL, it is useful to compare its binding capacity towards metal ions with that of peptides DAHK-Am (Asp-Ala-His-Lys-Amide) or DAH-Am, models for the amino-terminal site of albumin. Although this comparison is only approximate [40], however it allows to infer the potentiality of AGHLDDLPGALSAL to compete *in vivo* with albumin and with low molecular-weight ligands for binding metal ions. As for copper, such a comparison, which also includes the model tetrapeptide AGHL-Am, is shown in Fig. 10.

The presence of Asp residues seems to favor the first contact of AGHLDDLPGALSAL and DAHK-Am with Cu(II) at the most

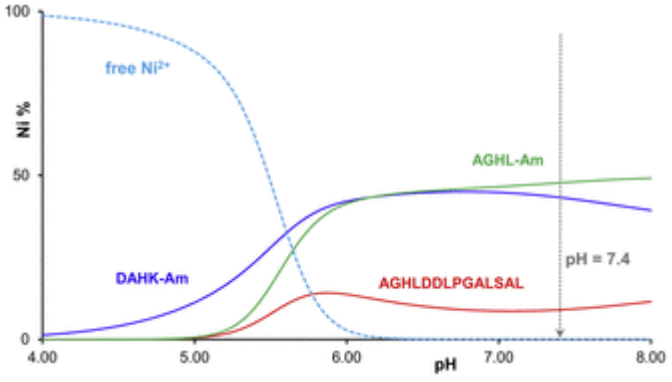

Fig. 11. Competition diagram calculated for a solution containing AGHLDDLPGALSAL, its short analogue AGHL-Am, the peptide DAHK-Am and Ni(II) in equimolar amounts. Stability constant data for DAHK-Am are taken from [40].

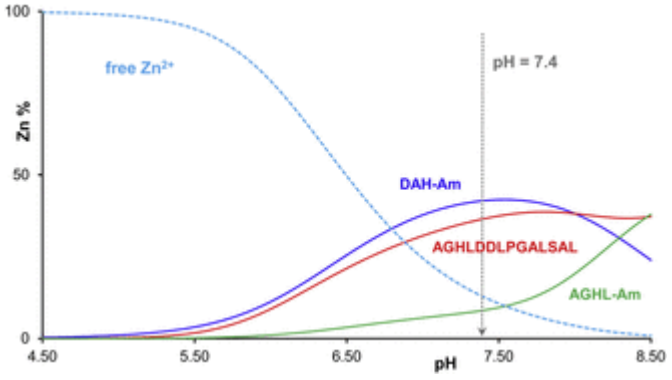

Fig. 12. Competition diagram calculated for a solution containing AGHLDDLPGALSAL, its short analogue AGHL-Am, the peptide DAH-Am and Zn(II) in equimolar amounts. Stability constant data for DAH-Am are taken from [39].

acidic pH values (3–4). From pH 4.5 onwards, the behaviors of DAHK-Am and AGHL-Am are very similar, while AGHLDDLPGALSAL is disadvantaged in the competition for binding Cu(II), over the entire acidic pH range. This could be due its bulkiness and/or to a greater difficulty by the metal to displace the amide protons of AGHLDDLPGALSAL, due to its considerable negative charge resulting from the presence of three deprotonated carboxyl groups. However, it is worth of note that, at physiological pH, the difference between the amounts of the complexes formed by AGHLDDLPGALSAL and DAHK-Am is small and not really significant, taking into account that this is an essentially qualitative comparison. This result suggests that AGHLDDLPGALSAL can effectively compete *in vivo* with albumin, which is present not only in the blood but also in the cerebrospinal fluid in a not negligible amount [41]. The competition will be especially effective in situations where there is high availability of Cu(II) (Fig. S7) or when AGHLDDLPGALSAL is in excess with respect to albumin itself (Fig. S8). This conclusion is also supported by the fact the K_d value found here for the Cu(II)/AGHLDDLPGALSAL system ($2.43 \cdot 10^{-14}$, Table 6) is two orders of magnitude lower than that reported for human albumin ($1.0 \cdot 10^{-12}$, at 298 K, pH = 7.4, I = 0.1 M (NaCl); Ref. [42]). Finally, considering as a competitor free His [43], one of the most important low-molecular-weight Cu(II) ligands in blood steam, we found that at physiological pH the distribution is completely in favor of AGHLDDLPGALSAL, as shown in Fig. S9. Also the biological assays made on cells *in vitro* support this conclusion, since AGHLDDLPGALSAL is clearly capable of sequestering most of the copper added to the culture medium, thus decreasing its toxicity against both cancer cells that human fibroblasts.

In the case of nickel, the situation presents both similarities and differences with respect to copper (Fig. 11). Similarly to Cu(II), the model peptide for albumin, DAHK-Am, proves to be able to bind the metal starting from the most acidic pH values; in addition, as in the case of copper, the behavior of DAHK-Am is very similar to that of AGHL-Am up to basic pH. However, as for AGHLDDLPGALSAL, this long peptide looks less effective than the shorter ones, in the whole explored pH range, without exception for the physiological pH in agreement with calculated K_d values of Table 6. It can be suggested that the steric hindrance plays here a more important role because of the more stringent geometric requirements for the formation of the square-planar Ni(II) complex.

Finally, as regards Zn(II), the only model peptide available in the literature to build up a competition diagram is the shorter DAH-Am [44]; however, the lack of the Lys residue should not significantly alter the meaning of the results. The competition diagram of Fig. 12 clearly shows a different behavior with respect to the other two metal ions. The importance of the role played by the carboxylate groups in both the model peptide DAH-Am and AGHLDDLPGALSAL to reinforce the coordination of the zinc to the two nitrogens of histidine and the terminal amine, is evident here. AGHL-Am, which does not possess any carboxyl group, forms significantly less stable zinc complexes at acid and neutral pH. However, at basic pH, where hydroxo-complexes are formed, the three ligands do not show any significant difference.

5. Conclusions

In this work we have studied for the first time the complexing properties of the peptide AGHLDDLPGALSAL, an endogenous fragment of the α-chain of hemoglobin, against some divalent metal ions of biological interest. The thermodynamic and spectroscopic parameters confirmed that AGHLDDLPGALSAL has the ability to form very stable complexes of the Cu(II) and Ni(II) ions, with an *albumin-like* coordination geometry, in virtue of the presence in its structure of the amino-terminal sequence called "ATCUN motif". The major species at physiological pH is the complex $[MLH_{-2}]^{3-}$ characterized by a square-planar geometry for nickel and a distorted octahedral structure for copper; the central metal ion is coordinated to four nitrogens of the ligand deriving from the imidazole of His, the amino-terminus and the two amide groups of the peptidic chain belonging to residues Gly and His. As far as zinc is concerned, this metal proved not able to displace the amide protons and to bind the nitrogens of the peptide backbone, with the consequence that its complexes are much less stable than those formed by the other two metals. Zinc forms mono- and bis-complexes, binding the two amino nitrogens of imidazole and terminal amine, with the possible participation of available carboxylate groups of Asp residues.

Finally, the biological assays have shown a definite protective activity of AGHLDDLPGALSAL against the cellular toxicity of Cu(II), towards both cancer cells and human fibroblasts.

All the results suggest that the chelating ability of AGHLDDLPGALSAL, especially towards the Cu(II) ion, can play an important role in the biological action of this peptide *in vivo*.

Abbreviations

AGHL-Am peptide Ala-Gly-His-Leu-Amide (protected at its C-terminus)	AGHLD-DLPGAL-SAL
unprotected peptide Ala-Gly-His-Leu-Asp-Asp-Leu-Pro-Gly-Ala-Leu-Ser-Ala-Leu	ATCUN
Amino Terminal Cu and Ni (binding motif)	DAH-Am
peptide Asp-Ala-His-Amide (protected at its C-ter-minus)	DAHK-Am
peptide Asp-Ala-His-Lys-Amide (protected at its C-terminus)	DMEM
Dulbecco's Modified Eagle Medium for cell culture	ESI-MS
Electrospray Ionization Mass Spectrometry	K_d
dissociation constant	MTT
3-(4,5-dimethylthiazol-2-yl)-2,5-diphenyltetra-zolium bromide	N_{am}
amide nitrogen	N_{im}
imidazole nitrogen	RPMI
Roswell Park Memorial Institute medium for cell culture	

Acknowledgements

The financial support of the University of Ferrara (FAR 2014) is gratefully acknowledged.

Appendix A. Supplementary data

Supplementary data to this article can be found online at http://dx.doi.org/10.1016/j.jinorgbio.2016.04.001.

References

[1] Z.W. Lai, A. Petrera, O. Schilling, Biol. Chem. 396 (2015) 185–192.
[2] S. Mahboob, A. Mohamedali, S.B. Ahn, P. Schulz-Knappe, E. Nice, M.S. Baker, J. Proteome 127 (2015) 300–309.
[3] I. Garreau, D. Chansel, S. Vandermeersch, I. Fruitier, J.M. Piot, R. Ardaillou, Peptides 19 (1998) 1339–1348.
[4] A.S. Heimann, L. Gomes, C.S. Dale, R.L. Pagano, A. Gupta, L.L. de Souza, A.D. Luchessi, L.M. Castro, R. Giorgi, V. Rioli, E.S. Ferro, L.A. Devi, Proc. Natl. Acad. Sci. U. S. A. 104 (2007) 20588–20593.
[5] N.M. Ribeiro, E.F. Toniolo, L.M. Castro, L.C. Russo, V. Rioli, E.S. Ferro, C.S. Dale, Peptides 48 (2013) 10–20.
[6] C. Harford, B. Sarkar, Acc. Chem. Res. 30 (1997) 123–130.
[7] D. Russino, E. McDonald, L. Hejazi, G.R. Hanson, C.E. Jones, Chem. Neurosci. 4 (2013) 1371–1381.
[8] N.L. Benoiton, Chemistry of Peptide Synthesis, Taylor & Francis, London, , 2005125–154.
[9] N.A. Solé, G. Barany, J. Org. Chem. 57 (1992) 5399–5403.
[10] H.M. Irving, M.G. Miles, L.D. Pettit, Anal. Chim. Acta 38 (1967) 475–488.
[11] P. Gans, B. O'Sullivan, Talanta 51 (2000) 33–37.
[12] P. Gans, A. Sabatini, A. Vacca, J. Chem. Soc. Dalton Trans. (1985) 1195–1200.
[13] G. Gran, Acta Chem. Scand. 4 (1950) 559–577.
[14] P. Gans, A. Sabatini, A. Vacca, Talanta 43 (1996) 1739–1753.
[15] H. Kozlowski, M. Luczkowski, M. Remelli, Dalton Trans. 39 (2010) 6371–6385.
[16] G. Crisponi, M. Remelli, Coord. Chem. Rev. 252 (2008) 1225–1240.
[17] L. Alderighi, P. Gans, A. Ienco, D. Peters, A. Sabatini, A. Vacca, Coord. Chem. Rev. 184 (1999) 311–318.
[18] C.F. Baes, R.E. Mesmer, The Hydrolysis of Cations, John Wiley & Sons, Ltd., New York, 1976.
[19] J. Powell Kipton, L. Brown Paul, H. Byrne Robert, T. Gajda, G. Hefter, A.-K. Leuz, S. Sjöberg, H. Wanner, Pure Appl. Chem. 85 (2013) 2249.
[20] M.B. Hansen, S.E. Nielsen, K. Berg, J. Immunol. Methods 119 (1989) 203–210.
[21] L.D. Pettit, H.K.J. Powell, The IUPAC Stability Constants Database, Royal Society of Chemistry, London, 1992-2000.
[22] H. Sigel, R.B. Martin, Chem. Rev. 82 (1982) 385–426.
[23] C. Conato, H. Kozlowski, P. Mlynarz, F. Pulidori, M. Remelli, Polyhedron 21 (2002) 1469–1474.
[24] R.W. Hay, M.M. Hassan, C. You-Quan, J. Inorg. Biochem. 52 (1993) 17–25.
[25] P. Mlynarz, D. Valensin, K. Kociolek, J. Zabrocki, J. Olejnik, H. Kozlowski, New J. Chem. 26 (2002) 264–268.
[26] E. Farkas, I. Sovago, T. Kiss, A. Gergely, J. Chem. Soc. Dalton Trans. (1984) 611–614.
[27] S. Lau, B. Sarkar, J. Chem. Soc. Dalton Trans. (1981) 491–494.
[28] T. Sakurai, A. Nakahara, Inorg. Chem. 19 (1980) 847–853.
[29] P.G. Daniele, E. Prenesti, O. Zerbinati, R. Aigotti, G. Ostacoli, Spectrochim. Acta A 49 (1993) 1373–1378.
[30] H.F. Stanyon, X. Cong, Y. Chen, N. Shahidullah, G. Rossetti, J. Dreyer, G. Papamokos, P. Carloni, J.H. Viles, FEBS J. 281 (2014) 3945–3954.
[31] P. Kolkowska, K. Krzywoszynska, S. Potocki, P.R. Chetana, M. Spodzieja, S. Rodziewicz-Motowidlo, H. Kozlowski, Dalton Trans. 44 (2015) 9887–9900.
[32] R.B. Martin, in: H. Sigel (Ed.), Metal Ions Biological Systems, Vol. 1, Marcel Dekker Inc., New York, 1974.
[33] R.B. Martin, in: H. Sigel, A. Sigel (Eds.), Metal Ions in Biological Systems, Vol. 23, Marcel Dekker Inc., New York, 1988.
[34] H. Kozlowski, A. Lebkiri, C.O. Onindo, L.D. Pettit, J.F. Galey, Polyhedron 14 (1995) 211–218.
[35] M. Rowinska-Zyrek, D. Witkowska, D. Valensin, W. Kamysz, H. Kozlowski, Dalton Trans. 39 (2010) 5814–5826.
[36] W. Bal, M. Sokołowska, E. Kurowska, P. Faller, Biochim. Biophys. Acta 1830 (2013) 5444–5455.
[37] S. Sjoberg, Pure Appl. Chem. 69 (1997) 1549–1570.
[38] R.P. Agarwal, D.D. Perrin, J. Chem. Soc. Dalton Trans. (1977) 53–57.
[39] P.G. Daniele, P. Amico, G. Ostacoli, M. Marzona, Ann. Chim. (Rome) 73 (1983) 299–313.
[40] M. Sokolowska, A. Krezel, M. Dyba, Z. Szewczuk, W. Bal, Eur. J. Biochem. 269 (2002) 1323–1331.
[41] H. Reiber, Clin. Chim. Acta 310 (2001) 173–186.
[42] M. Rozga, M. Sokolowska, A.M. Protas, W. Bal, J. Biol. Inorg. Chem. 12 (2007) 913–918.
[43] G. Borghesani, F. Pulidori, M. Remelli, R. Purrello, E. Rizzarelli, J. Chem. Soc. Dalton Trans. (1990) 2095–2100.
[44] P.G. Daniele, P. Amico, G. Ostacoli, M. Marzona, Ann. Chim. 73 (1983) 299–313.